

Off-diagonal correlations of the Calogero-Sutherland model

G.E. Astrakharchik,^{1,2} D.M. Gangardt,³ Yu.E. Lozovik,² and I.A. Sorokin²

¹*Dipartimento di Fisica, Università di Trento and BEC-INFM, I-38050 Povo, Italy*

²*Institute of Spectroscopy, 142190 Troitsk, Moscow region, Russia*

³*Laboratoire de Physique Théorique et Modèles Statistiques, Université Paris Sud, 91405 Orsay Cedex, France*

(Dated: September 25, 2019)

We study correlation functions of the Calogero-Sutherland model in the whole range of the interaction parameter. Using the replica method we obtain analytical expressions for the long-distance asymptotics of the one-body density matrix in addition to the previously derived asymptotics of the pair-distribution function [D.M. Gangardt and A. Kamenev, Nucl. Phys. B, **610**, 578 (2001)]. The leading analytic and non-analytic terms in the short-distance expansion of the one-body density matrix are discussed. Numerical results for these correlation functions are obtained using Monte Carlo techniques for all distances. The momentum distribution and static structure factor are calculated. The potential and kinetic energies are obtained using the Hellmann-Feynman theorem. Perfect agreement is found between the analytical expressions and numerical data. These results allow for the description of physical regimes of the Calogero-Sutherland model. The zero temperature phase diagram is found to be of a crossover type and includes quasi-condensation, quasi-crystallization and quasi-supersolid regimes.

I. INTRODUCTION

There is an ongoing interest in correlation properties of the Calogero-Sutherland model (CSM). From the theoretical perspective the Calogero-Sutherland model provides a rare example of exactly solvable model with relatively simple structure of eigenstates. In the present work we address the question of coherence properties of the CSM measured by the off-diagonal correlation functions. Our study complements the previous results on the diagonal density-density correlation properties of the CSM and allows to draw conclusions about the coexistence of both types of long-range correlations in an appropriate interval of the interaction parameter.

Introduced in Ref. [1], the CSM describes a system of particles interacting with a scale-free potential, which is inversely proportional to the square of the distance between particles. The ground state wave function was shown to have a form which is factorizable over pairs of particles. Each factor is proportional to $(x_i - x_j)^\lambda$ with x_i, x_j being the coordinates of particles forming a pair and the parameter λ being directly related to the interaction strength. In addition to the convenient description of the excitations in terms of non-interacting particles with fractional statistics [2], this particular form of the ground state suggested a possibility to study correlations functions of this model.

Indeed, it was noted in [1] that for three special values $\lambda = 1/2, 1$ and 2 the ground state probability of the CSM coincides with the probability distribution of the eigenvalues of unitary random matrices, so the early results of Dyson [3] describe the static density correlations in the CSM. The analogy with random matrix theory allows also the calculation of dynamical density correlations [4] and dynamical Green's function [5, 6]. To deal with other values of interactions the Jack polynomial method has been applied to find correlation functions for integer [7] and rational [8] values of λ . The common drawback of these methods for a rational $\lambda = p/q$ is that the final expression for the correlation function is usually given as a sum over fractional excitations involving $p + q$ particle and hole quantum numbers, which goes over $p + q$ integrals in the thermodynamic limit. Such a decomposition makes the result appear as a highly irregular function of the coupling constant λ , leaving little hope of approaching its irrational values.

Recently, there has been success [9] in obtaining the density-density correlation functions of the CSM for arbitrary coupling λ , leading to transparent asymptotic expressions in the long-distance limit. Based on the replica method from the theory of disordered systems, this approach involves the representation of the correlation functions using a duality transformation as an m -dimensional integral with eventual analytic continuation in m . Similar methods were applied recently [10] to study off-diagonal correlations of one-dimensional impenetrable bosons, equivalent to the bosonic CSM for one specific value of $\lambda = 1$.

In this paper we extend the replica method for studying the off-diagonal correlations (equal-time Green's function) and corresponding momentum distributions. The main result is the exact long-distance asymptotic behaviour of the one-body density matrix in the form of the Haldane's universal hydrodynamic expansion [11]. We consider both bosonic and fermionic statistics of the particles encoded in the symmetry of the wavefunctions using the definitions of the original work of Sutherland [1] (see also [5]). Being irrelevant for the density correlations, the quantum statistics affects drastically the results for the off-diagonal correlations.

In addition, we study the short-distance behaviour of the one-body density matrix and find several leading terms (analytic and non-analytic) in the short-distance expansion. The latter is directly related to the high-momentum tails

of the momentum distribution. The short-distance (high momentum) physics enters the expressions for potential and kinetic energies which we calculate as a function of interactions by using the Hellmann-Feynman theorem.

To check our predictions we use a Monte Carlo method to calculate numerically the correlation functions for arbitrary distances and different values of the interaction parameter. The advantage of the Calogero-Sutherland model is that its ground state wavefunction is known explicitly and can be easily sampled by Metropolis algorithm. This permits us to obtain unambiguous results for intermediate distances, where analytical methods fail.

Combining these results with previous knowledge of the diagonal two-body correlations (pair distribution function) [9] allows us to describe different physical regimes of the CSM at zero temperature. In particular, we discuss long- and short-range order as a function of the coupling constant λ for diagonal and off-diagonal correlations. Since the true long-range order is absent in one dimension, we define it through the correlation function of the (local) order parameter which has the slowest power-law decay and use the word “quasi” to stress this peculiarity of one dimension. We propose a phase diagram which describes (in order of increasing interaction strength) the crossover between three physical regimes: the quasi-condensate, quasi-supersolid and quasi-crystal.

The paper is organized as follows. In Section II we introduce the Hamiltonian of the Calogero-Sutherland model, its solution for the ground state and define correlation functions of interest. In Section III we present the calculation of the one-body density matrix based on the replica method and discuss the thermodynamic limit in Section IV. Results for the short-distance behaviour of the one-body density matrix and discussion of the kinetic and potential energies are found in Section V. Section VI is devoted to numerical Monte Carlo simulations and discussion of the physics of the CSM. In section VII we propose the phase diagram of the CSM and draw our conclusions. Appendix A contains mathematical details of our calculations.

II. THE CALOGERO-SUTHERLAND MODEL

We consider a finite system of N particles of mass m on a ring of length L . The Hamiltonian of the Calogero-Sutherland model is given by the sum of the kinetic energy and pair interactions controlled by parameter λ :

$$H = \frac{\hbar^2}{2m} \left[- \sum_{i=1}^N \frac{\partial^2}{\partial x_i^2} + \lambda(\lambda-1) \sum_{i \neq j} \frac{\pi^2/L^2}{\sin^2(\pi(x_i - x_j)/L)} \right]. \quad (1)$$

The interaction between two particles on the ring is inversely proportional to square of the chord distance between them. It becomes an inverse square potential in the thermodynamic limit.

The ground state wave function of the Hamiltonian (1) was found in [1] and can be written as:

$$\Phi(x_1, \dots, x_N) = C_N(\lambda) \prod_{k < l} \left(e^{2\pi i x_k/L} - e^{2\pi i x_l/L} \right)^\lambda. \quad (2)$$

Here $C_N(\lambda)$ is the normalization constant given by

$$C_N^2(\lambda) = \frac{1}{L^N} \frac{\Gamma(1+\lambda)^N}{\Gamma(1+\lambda N)}. \quad (3)$$

The expression (2), as it stands, is valid only for a particular ordering of particles, for instance $x_1 < x_2 < \dots < x_N$. To extend the expression (2) to other ordering configuration one has to specify the quantum statistics (bosonic or fermionic) of the particles. We modify the expression (2) to take into account the symmetry under permutation of the particle coordinates

$$\Phi_{B,F}(x_1, \dots, x_N) = C_N(\lambda) \prod_{k < l} \left| e^{2\pi i x_k/L} - e^{2\pi i x_l/L} \right|^\lambda S_{B,F}, \quad (4)$$

by introducing the factor $S_{B,F}$ such that for bosons $S_B = 1$, while for fermions $S_F = (-1)^P$ is the parity of the permutation P , where $x_{P_1} < x_{P_2} < \dots < x_{P_N}$. As we shall see different quantum statistics of particles is crucial for off-diagonal correlations, which was already noted in the context of the Calogero-Sutherland model in early works [1].

The main quantity of interest is the one-body density matrix which in terms of the ground state wave function is written as

$$g_1^{B,F}(x-y) = N \int_0^L d^{N-1}x \Phi_{B,F}^*(x_1, \dots, x_{N-1}, x) \Phi_{B,F}(x_1, \dots, x_{N-1}, y). \quad (5)$$

Due to the translational invariance in a homogeneous system the one-body density matrix is a function of the difference $x - y$ only. Knowledge of the one-body density matrix enables one to calculate the momentum distribution as the Fourier transform:

$$n_k = \int dx e^{-ikx} g_1(x). \quad (6)$$

The one-body density matrix has dimensions of density and is normalized so that $g_1(0) = n$, where $n = N/L$ is the particle density. The momentum distribution n_k is dimensionless, it is defined for $k_l = 2\pi l/L$, where l is an integer, and is normalized to the total number of particles $\sum_k n_k = Lg_1(0) = N$.

In addition to the off-diagonal correlation functions we consider the two-body density matrix (pair distribution function). It is defined as

$$g_2(x - y) = N(N - 1) \int d^{N-2}x |\Phi(x_1, \dots, x_{N-2}, x, y)|^2. \quad (7)$$

The static structure factor is related to $g_2(x)$:

$$S_k = 1 + \frac{1}{n} \int dx e^{-ikx} (g_2(x) - n^2). \quad (8)$$

The two-body density matrix has dimensions of density squared and is normalized so that $\lim_{x \rightarrow \infty} g_2(x) = n^2$, while the static structure factor is a dimensionless quantity and $\lim_{k \rightarrow \infty} S_k = 1$. It is independent of statistics, as it involves only the absolute value of the ground state wavefunction. In the next section we calculate analytically the one-body density matrix (5). The results for the pair distribution function (7) were obtained in [9] and we reproduce them in the Section VID.

III. ONE-BODY DENSITY MATRIX

To calculate the one-body density matrix we define the dimensionless function $G_1(\alpha)$ such that $g_1(x) = nG_1(2\pi x/L)$ and $G_1(0) = 1$. Factorizing the ground state wave function (4) we rewrite the definition (5) in the form of the average

$$G_1(\alpha) = \frac{\Gamma(\lambda)\Gamma(1 + \lambda N)}{2\pi\Gamma(\lambda(1 + N))} \left\langle \prod_{j=1}^N |1 - e^{i\theta_j}|^\lambda |e^{i\alpha} - e^{i\theta_j}|^\lambda \right\rangle_{N,\lambda}, \quad (9)$$

where the average is defined as

$$\langle f(e^{i\theta_1}, e^{i\theta_2}, \dots, e^{i\theta_N}) \rangle_{N,\lambda} = \frac{\Gamma^N(1 + \lambda)}{\Gamma(1 + \lambda N)} \int_0^{2\pi} \frac{d^N\theta}{(2\pi)^N} |\Delta_N(e^{i\theta})|^{2\lambda} f(e^{i\theta_1}, e^{i\theta_2}, \dots, e^{i\theta_N}), \quad (10)$$

and $\Delta_N(z)$ is the Vandermonde determinant

$$\Delta_N(z) = \Delta(z_1, z_2, \dots, z_N) = \prod_{i < j} (z_i - z_j). \quad (11)$$

Here we have changed the number of particles from N to $N + 1$ in order to deal with N dimensional integrals. This difference does not matter in the thermodynamic limit, and for the finite system we will restore the correct number of particles in the final expressions.

To calculate the average in (9) we use the replica trick, along the lines of the calculation in [9] and [10]. Namely, consider the following function

$$Z_m^{(\lambda)}(\alpha) = \left\langle \prod_{j=1}^N (1 - e^{i\theta_j})^m (e^{i\alpha} - e^{i\theta_j})^m \right\rangle_{N,\lambda}. \quad (12)$$

It can be shown along the lines of [12] that $G_1(\alpha)$ is obtained from $Z_m^{(\lambda)}(\alpha)$ by the analytical continuation $m \rightarrow \lambda$. Later we discuss this procedure in some detail and show how the quantum statistics of the particles, bosonic or fermionic, appears naturally in our calculations. For the moment we take advantage of the duality transformation

[13], which enables one to re-express the N -dimensional integral (12) depending on the parameter m as a m -dimensional integral depending on N as a parameter:

$$Z_m^{(\lambda)}(t) = \frac{e^{-iNm\alpha/2}}{S_m(1/\lambda)} \int_0^1 d^m x |\Delta_m(x)|^{\frac{2}{\lambda}} \prod_{a=1}^m x_a^{\frac{1}{\lambda}-1} (1-x_a)^{\frac{1}{\lambda}-1} (1-(1-e^{i\alpha})x_a)^N. \quad (13)$$

The duality $\lambda \leftrightarrow 1/\lambda$ becomes evident by comparing the power of Vandermonde determinants in Eqs. (10), (12) and (13). We put $Z_m^{(\lambda)}(0) = 1$, so the normalization constant is given by the Selberg integral:

$$S_m(1/\lambda) = \int_0^1 d^m x |\Delta_m(x)|^{\frac{2}{\lambda}} \prod_{a=1}^m x_a^{\frac{1}{\lambda}-1} (1-x_a)^{\frac{1}{\lambda}-1} = \prod_{a=1}^m \frac{\Gamma^2\left(\frac{a}{\lambda}\right) \Gamma\left(1+\frac{a}{\lambda}\right)}{\Gamma\left(1+\frac{1}{\lambda}\right) \Gamma\left(\frac{m+a}{\lambda}\right)}. \quad (14)$$

The dual representation is an excellent starting point for the asymptotic expansion in the large N limit. In this limit the main contribution to the integral over each variable x_a comes from the limits of integration $x_+ = 1$ and $x_- = 0$, so we expand close to these points:

$$x_a = x_- + \frac{\xi_a}{N(1-e^{i\alpha})}, \quad a = 1, \dots, l \quad (15)$$

$$x_b = x_+ - \frac{\xi_b}{N(1-e^{-i\alpha})}, \quad b = l+1, \dots, m. \quad (16)$$

To the leading order in N the stationary action is

$$(1 - (1 - e^{i\alpha})x_a)^N = \begin{cases} e^{-\xi_a}, & a = 1, \dots, l \\ e^{iN\alpha} e^{-\xi_a}, & a = l+1, \dots, m \end{cases}, \quad (17)$$

and the Vandermonde determinants factorize as

$$\Delta_m(x) \simeq \left(\frac{1}{N(1-e^{i\alpha})} \right)^{l(l-1)/2} \left(\frac{1}{N(1-e^{-i\alpha})} \right)^{(m-l)(m-l-1)/2} \Delta_l(\xi_a) \Delta_{m-l}(\xi_b), \quad (18)$$

which allows the calculation of the remaining fluctuation contributions in the form of the Selberg integrals [14] as follows

$$I_l(1/\lambda) = \int_0^1 d^l \xi |\Delta_l(\xi)|^{\frac{2}{\lambda}} \prod_{a=1}^l \xi_a^{\frac{1}{\lambda}-1} e^{-\xi_a} = \prod_{a=1}^l \frac{\Gamma\left(\frac{a}{\lambda}\right) \Gamma\left(1+\frac{a}{\lambda}\right)}{\Gamma\left(1+\frac{1}{\lambda}\right)}. \quad (19)$$

Collecting factors arising from the change of variables (16) and summing over all 2^m saddle points yields the following result:

$$Z_m^{(\lambda)}(\alpha) = \sum_{l=0}^m (-1)^{\frac{m}{\lambda}(\frac{m}{2}-l)} H_m^l(\lambda) \frac{e^{i(N+\frac{m}{\lambda})(\frac{m}{2}-l)\alpha}}{(2N \sin \frac{\alpha}{2})^{\frac{l^2+(m-l)^2}{\lambda}}}, \quad (20)$$

where the factors

$$H_m^l(\lambda) = \binom{m}{l} \frac{I_l(1/\lambda) I_{m-l}(1/\lambda)}{S_m(1/\lambda)} \quad (21)$$

include the combinatorial factor arising from the number of ways to choose l variables x_a close to one saddle point, x_- say, and $m-l$ variables x_b in the vicinity of the other saddle point. Having established the asymptotic expression (20) valid for integer m we consider separately the analytic continuation $m \rightarrow \lambda$ for bosons and fermions.

A. Bosonic statistics

To obtain the bosonic one-body density matrix one should treat m as an *even integer* before taking the limit $m \rightarrow \lambda$. In this case the main contribution to the sum (20) comes from the central point $l = m/2$. It behaves as $(N \sin(\alpha/2))^{-m^2/2\lambda}$ and substituting $m = \lambda$ yields the result expected from the conformal field theory $G_1 \sim$

$(N \sin(\alpha/2))^{-\lambda/2}$. To perform analytic continuation we rearrange the sum by changing the summation index $l = m/2 + k$ and letting k run from $-\infty$ to $+\infty$. The coefficient of the dominant ($k = 0$) term is given by $A_\lambda^2(\lambda) = \lim_{m \rightarrow \lambda} H_m^{m/2}$. The analytic continuation of this expression is described in detail in Appendix A. The result is

$$A_\lambda(\lambda) = \frac{\Gamma^{1/2}(1+\lambda)}{\Gamma(1+\lambda/2)} \exp \int_0^\infty \frac{dt}{t} e^{-t} \left(\frac{\lambda}{4} - \frac{2(\cosh \frac{t}{2} - 1)}{(1 - e^{-t})(e^{t/\lambda} - 1)} \right). \quad (22)$$

The coefficients $D_k^2(\lambda) = \lim_{m \rightarrow \lambda} H_m^{m/2+k} / H_m^{m/2}$ of the oscillating $k \neq 0$ terms are obtained straightforwardly:

$$D_k(\lambda) = \lim_{m \rightarrow \lambda} \prod_{a=1}^k \frac{\Gamma\left(\frac{m/2+a}{\lambda}\right)}{\Gamma\left(\frac{m/2+1-a}{\lambda}\right)} = \prod_{a=1}^k \frac{\Gamma\left(\frac{1}{2} + \frac{a}{\lambda}\right)}{\Gamma\left(\frac{1}{2} + \frac{1}{\lambda} - \frac{a}{\lambda}\right)} \quad (23)$$

and can be calculated recursively

$$D_1(\lambda) = \frac{\Gamma\left(\frac{1}{2} + \frac{1}{\lambda}\right)}{\Gamma\left(\frac{1}{2}\right)}, \quad D_{k+1}(\lambda) = \frac{\Gamma\left(\frac{1}{2} + \frac{1}{\lambda} + \frac{k}{\lambda}\right)}{\Gamma\left(\frac{1}{2} - \frac{k}{\lambda}\right)} D_k(\lambda). \quad (24)$$

The correlation function is thus represented as a sum of one smooth component and oscillatory corrections due to the short-distance correlations:

$$G_1^B(\alpha) \sim \frac{A_\lambda^2(\lambda)}{|2X|^{\lambda/2}} \left(1 + 2 \sum_{k=1}^{\infty} (-1)^k D_k^2(\lambda) \frac{\cos(kN\alpha)}{|2X|^{2k^2/\lambda}} \right). \quad (25)$$

Here we have changed the number of particles back to N , and defined $X = (N-1) \sin \frac{\alpha}{2}$. From the last expression one sees that if λ is an even integer the infinite sum in the expression (25) becomes finite. For $\lambda = 2n$ the correlation function contains only n oscillatory components.

B. Fermionic statistics

To deal with fermions, m has to be considered as an *odd integer* prior to the limiting procedure $m \rightarrow \lambda$. In this case the dominant contribution to the sum (20) comes from the terms $l = (m \pm 1)/2$, which being combined together for $m \rightarrow \lambda$ lead to the oscillating behaviour $\sim 2 \sin(\frac{1}{2}(N+1)\alpha) / ((2N \sin(\alpha/2))^{\lambda/2+1/2\lambda})$ of the one-body density matrix. This behaviour is again in complete agreement with the conformal field theory. The coefficient of this term $C_\lambda^2(\lambda) = \lim_{m \rightarrow \lambda} H_m^{(m+1)/2}$ is calculated by an analytic continuation as explained in Appendix A. The result is

$$C(\lambda) = \Gamma^{1/2}(\lambda) \frac{\Gamma(1/2 + 1/2\lambda)}{\Gamma(1/2 + \lambda/2)} \exp \int_0^\infty \frac{dt}{t} e^{-t} \left(\frac{\lambda}{4} - \frac{1}{4\lambda} + \frac{2e^{t/2\lambda} (\cosh \frac{t}{2\lambda} - \cosh \frac{t}{2})}{(1 - e^{-t})(e^{t/\lambda} - 1)} \right). \quad (26)$$

and the coefficients $F_k^2(\lambda) = \lim_{m \rightarrow \lambda} H_m^{(m+k)/2} / H_m^{(m+1)/2}$ are given by

$$F_k(\lambda) = \left(\frac{\lambda^2 - (2k-1)^2}{\lambda^2 - 1} \right)^{\frac{1}{2}} \prod_{a=1}^{k-1} \frac{\Gamma\left(1 + \frac{1+2a}{\lambda}\right)}{\Gamma\left(1 + \frac{1-2a}{\lambda}\right)}, \quad (27)$$

or by the recursion relation

$$F_1(\lambda) = 1, \quad F_{k+1}(\lambda) = \left(\frac{\lambda^2 - (2k+1)^2}{\lambda^2 - (2k-1)^2} \right)^{\frac{1}{2}} \frac{\Gamma\left(1 + \frac{1+2k}{\lambda}\right)}{\Gamma\left(1 + \frac{1-2k}{\lambda}\right)} F_k(\lambda). \quad (28)$$

Restoring the number of particles and using $X = (N-1) \sin \frac{\alpha}{2}$, the fermionic one-body density matrix is finally given by a sum of oscillatory terms:

$$G_1^F(\alpha) \sim \frac{C^2(\lambda)}{|2X|^{\frac{\lambda}{2} + \frac{1}{2\lambda} - 1}} \frac{1}{X} \sum_{k=1}^{\infty} (-1)^{k-1} F_k^2(\lambda) \frac{\sin((k-1/2)N\alpha)}{|2X|^{2k(k-1)/\lambda}}. \quad (29)$$

For $\lambda = 2n-1$ the total number of terms in the sum is n .

IV. THERMODYNAMIC LIMIT

We now take the thermodynamic limit of the above expressions by recalling that $\alpha = 2\pi x/L$ so that $X = N \sin(\pi x/L) \simeq \pi x N/L = \pi n x = k_F x$ in the limit of infinite N and L . Here we have also defined $k_F = \pi n$, the Fermi momentum by analogy with free one-dimensional spinless fermions. In the thermodynamic limit the expressions (25) and (29) become:

$$\frac{g_1^B(x)}{n} \simeq \frac{A^2(\lambda)}{|2k_F x|^{\lambda/2}} \left(1 + 2 \sum_{m=1}^{\infty} (-1)^m \frac{D_m^2(\lambda) \cos 2mk_F x}{|2k_F x|^{2m^2/\lambda}} \right) \quad (30)$$

$$\frac{g_1^F(x)}{n} \simeq \frac{C^2(\lambda)}{|2k_F x|^{\frac{\lambda}{2} + \frac{1}{2\lambda} - 1}} \frac{1}{k_F x} \sum_{m=1}^{\infty} (-1)^{m-1} \frac{F_m^2(\lambda) \sin(2m-1)k_F x}{(2k_F x)^{2m(m-1)/\lambda}}. \quad (31)$$

These expressions agree completely with the results of Haldane based on the universal hydrodynamic theory for compressible quantum fluids [11]. The power-law universal decay of correlations with the distance provides the value of the corresponding Luttinger parameter $K = 1/\lambda$. The coefficients $A(\lambda)$ (22), $D_m(\lambda)$ (23) for bosons and $C(\lambda)$ (26), $F_m(\lambda)$ (27) for fermions, are model-specific non-universal numbers. Here they are obtained exactly for the Calogero-Sutherland model for the first time.

From the expressions (30), (31) we extract the singular behaviour of the momentum distribution using the definition (6). For bosons, the leading term in (30) yields the leading divergence for small momenta:

$$n_k \simeq \frac{2^\alpha}{\pi} A^2(\lambda) \Gamma(\alpha) \cos \frac{\pi\alpha}{2} \left| \frac{k}{k_F} \right|^{-\alpha}, \quad (32)$$

where the critical exponent $\alpha = \alpha(\lambda)$ is defined as $\alpha = 1 - \lambda/2$. This result is valid for $0 < \lambda < 2$, so that $0 < \alpha < 1$. For the special value of $\lambda = 1$, which corresponds to the system of impenetrable bosons [15] we have $\alpha = 1/2$. For the value $\lambda = 1/2$ Sutherland [5] was using a numerical estimate to suggest $\alpha = 1/\sqrt{2} = 0.707\dots$. We report here the exact value $\alpha = 3/4$. For $\lambda = 2$ the critical exponent $\alpha = 0$ is consistent with the logarithmic divergence found in [1]. The oscillating terms in (30) contribute to the weaker singularities at the points $k = \pm 2k_F, \pm 4k_F, \dots$

For fermions, due to the oscillating character of the one-body density matrix the dominant singularities appear at $k = \pm k_F$. The leading behaviour is extracted from the first term in (31). For $k \rightarrow k_F$ we have

$$n_k - \frac{1}{2} \simeq \frac{2^{-\beta} C^2(\lambda)}{\pi\beta} \Gamma(1-\beta) \cos \left(\frac{\pi(\beta-1)}{2} \right) \left| \frac{k - k_F}{k_F} \right|^\beta \text{sgn}(k_F - k) \quad (33)$$

and similarly for $k \rightarrow -k_F$. The critical exponent is defined as $\beta = \beta(\lambda) = \beta(1/\lambda) = \lambda/2 + 1/2\lambda - 1$, so that the power law behaviour of the momentum distribution is the same for λ and $1/\lambda$. The result (33) is valid for $0 < \beta < 1$ which implies $2 - \sqrt{3} < \lambda < 2 + \sqrt{3}$. For $\lambda = 1$ we have free fermions and $\beta(1) = 0$ corresponding to the Fermi-Dirac distribution. In other the special cases we have $\beta(1/2) = \beta(2) = 1/4$. Additional singularities exist at $k = \pm 3k_F, \pm 5k_F, \dots$

V. SHORT-DISTANCE CORRELATIONS OF THE CALOGERO-SUTHERLAND MODEL

The results in the previous section provide the long-distance behaviour of the one-body density matrix for the Calogero-Sutherland model and consequently the small-momenta behaviour of its momentum distribution. It is also possible to extract the short-distance properties of this model. We use the method introduced by Olshanii and Dunjko [16] to relate the tails of the momentum distribution to singularities of the wave function. To present this method we consider bosonic statistics and discuss later the corresponding modifications for fermions.

The momentum distribution (6) is rewritten in the following form:

$$n_k = n \int dx_2 \dots dx_N |\Phi(k, x_2, \dots, x_N)|^2, \quad (34)$$

where we have defined the Fourier transform of the ground state wave function (2) with respect to its first coordinate:

$$\begin{aligned} \Phi(k, x_2, \dots, x_N) &= \int_0^L dx e^{-ikx} \Phi(x, x_2, \dots, x_N) \\ &= C_N(\lambda) \prod_{2 \leq k < l \leq N} \left| e^{2\pi x_k/L} - e^{2\pi x_l/L} \right|^\lambda \int_0^L dx e^{-ikx} \prod_{l=2}^N \left| e^{2\pi x/L} - e^{2\pi x_l/L} \right|^\lambda. \end{aligned} \quad (35)$$

The remaining integral can be evaluated using the following property of Fourier transforms. Let $f(z)$ have a singularity of the form $f(z) = |z - z_0|^\alpha g(z)$ where $g(z)$ is regular at $z = z_0$ and $\alpha > -1$, $\alpha \neq 0, 2, 4, \dots$. Then

$$\int_{-\infty}^{+\infty} dz e^{-ipz} f(z) = 2 \cos\left(\frac{\pi(\alpha+1)}{2}\right) \Gamma(1+\alpha) \frac{g(z_0) e^{-ipz_0}}{|p|^{\alpha+1}} + O\left(\frac{1}{p^{\alpha+2}}\right). \quad (36)$$

If $f(z)$ has several singularities, then the right hand side equals the sum of the corresponding contributions. Using this fact and (36) the large- k behaviour of the wave function (35) is determined by the singularities at the positions of the remaining particles:

$$\begin{aligned} \Phi(k, x_2, \dots, x_N) &\simeq \frac{2}{|k|^{\lambda+1}} \left(\frac{2\pi}{L}\right)^\lambda \cos\left(\frac{\pi(\lambda+1)}{2}\right) \Gamma(1+\lambda) C_N(\lambda) \prod_{2 \leq k < l \leq N} \left| e^{2\pi x_k/L} - e^{2\pi x_l/L} \right|^\lambda \\ &\times \sum_{j=2}^N e^{-ikx_j} \prod_{l \neq j} \left| e^{2\pi x_j/L} - e^{2\pi x_l/L} \right|^\lambda. \end{aligned} \quad (37)$$

Substituting this expansion into (34) and keeping only k -independent diagonal terms in the double sum leads to the following result for the asymptotic behaviour of the momentum distribution:

$$n_k \simeq K_N(\lambda) \left| \frac{k_F}{k} \right|^{2+2\lambda}, \quad (38)$$

with the constant $K_N(\lambda)$ defined by the following average in the ground state of $N-1$ particles:

$$\begin{aligned} K_N(\lambda) &= \frac{2^{2+2\lambda}}{\pi^2} \cos^2\left(\frac{\pi(\lambda+1)}{2}\right) \frac{\Gamma^3(1+\lambda) \Gamma(1-\lambda+\lambda N)}{N^{2\lambda} \Gamma(1+\lambda N)} \\ &\times \int dx_2 \dots dx_N |\Phi(x_2, \dots, x_N)|^2 \prod_{l=3}^N \left| e^{2\pi x_2/L} - e^{2\pi x_l/L} \right|^{2\lambda}. \end{aligned} \quad (39)$$

The result (38) is valid also for fermions for $\lambda \neq 1, 3, \dots$, with a modification of the proportionality constant:

$$\tilde{K}_N(\lambda) = \tan^2\left(\frac{\pi(\lambda+1)}{2}\right) K_N(\lambda). \quad (40)$$

The result (38) suggests the following short range expansion for the one-body density matrix as a sum of analytic and non-analytic functions:

$$\begin{aligned} \frac{g_1(x)}{n} &= 1 + c_1(\lambda) k_F x + \frac{c_2(\lambda)}{2!} (k_F x)^2 + \frac{c_3(\lambda)}{3!} (k_F x)^3 + \dots \\ &+ a(\lambda) |k_F x|^{1+2\lambda} + O(|k_F x|^{2+2\lambda}). \end{aligned} \quad (41)$$

The coefficients $c_l(\lambda)$ in the Taylor expansion of the analytic part of g_1 are the corresponding moments of the momentum distribution

$$c_l(\lambda) = \frac{i^l}{n^l} \int \frac{dk}{2\pi n} k^l n_k. \quad (42)$$

Due to the time-reversal symmetry the momentum distribution is an even function, $g_1(x)$ is real and odd moments vanish. The non-analytic part of the one-body density matrix starts as $|x|^{2\lambda+1}$ with the coefficient which can be related to the high-momentum tails (38) using (36):

$$a(\lambda) = \frac{\pi K_N(\lambda)}{2 \cos(\pi(1+\lambda)) \Gamma(2+2\lambda)}. \quad (43)$$

Non-analyticity of the density matrix at $x = 0$ reflects the fact seen already from (38) that the l -th moment $c_l(\lambda)$ diverges for $l > 2\lambda + 1$.

Provided they exist, the moments c_{2l} are the same for bosons and fermions, a fact noticed by Sutherland in [5]. Therefore for sufficiently large λ the fermionic and bosonic one-body density matrices have the same leading Taylor

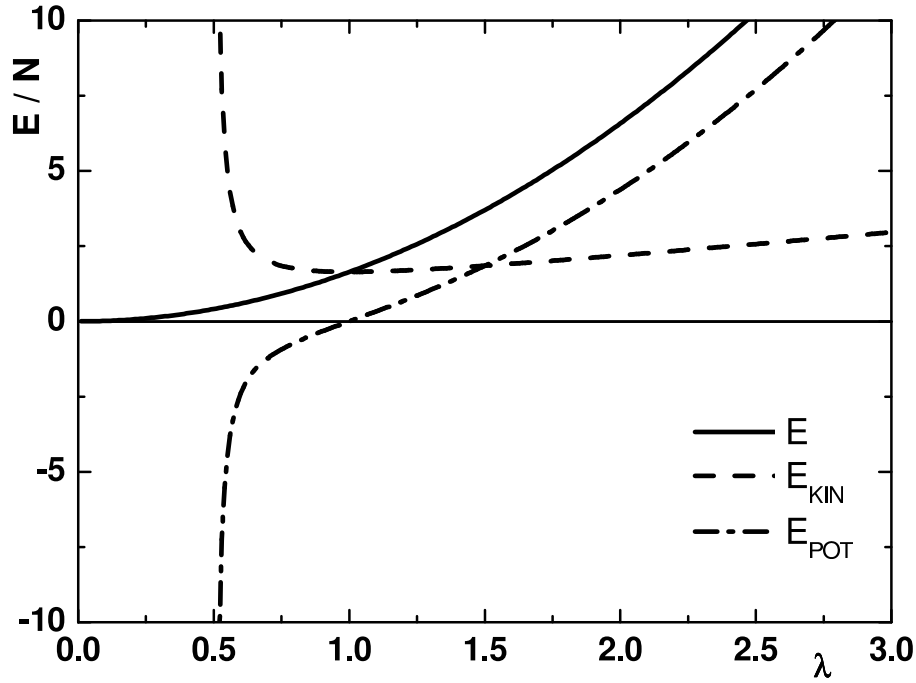


FIG. 1: Ground state energy of the CSM as a function of the interaction parameter λ : solid line – total energy per particle (44), dashed line – kinetic energy per particle (46), dot-dashed line – potential energy per particle (45). Energies are measured in units of $\hbar^2 n^2/m$.

expansion. This fact is easily explained on physical grounds, noticing that the strong repulsion prevents all exchange effects and particles do not “feel” the quantum statistics.

The second moment $c_2(\lambda)$ can be calculated explicitly since it is given by minus the kinetic energy per particle (in units of the Fermi energy). To obtain it one uses the Hellman-Feynman theorem to extract the potential energy from the dependence of the total energy on the strength of the particle-particle interaction. The ground state energy of the Calogero-Sutherland Hamiltonian (1) is known exactly [1] and is equal to

$$\frac{E}{N} = \frac{\langle H \rangle}{N} = \frac{\pi^2 \lambda^2}{6} \frac{\hbar^2 n^2}{m}. \quad (44)$$

We note that the potential energy is linear in $g = \lambda(\lambda - 1)$ and can be obtained by differentiating the ground state energy:

$$\frac{E_{pot}}{N} = \frac{g}{N} \left\langle \frac{\partial}{\partial g} H \right\rangle = \frac{g}{N} \frac{\partial}{\partial g} \langle H \rangle = \frac{\pi^2 \lambda^2 (\lambda - 1)}{3(2\lambda - 1)} \frac{\hbar^2 n^2}{m}, \quad \lambda > 1/2. \quad (45)$$

The kinetic energy is then obtained as a difference of the total ground state energy (44) and potential energy (45):

$$\frac{E_{kin}}{N} = \frac{E - E_{pot}}{N} = \frac{\pi^2 \lambda^2}{6(2\lambda - 1)} \frac{\hbar^2 n^2}{m}, \quad \lambda > 1/2. \quad (46)$$

Finally, for the second moment c_2 we obtain the following expression:

$$c_2 = -\frac{\lambda^2}{3(2\lambda - 1)}. \quad (47)$$

We plot the total, kinetic and potential energies in Fig. 1. The total energy is always positive and the compressibility also remains positive so that the system is (thermo-) dynamically stable. The case $\lambda > 1$ corresponds to repulsion between fermions while for $\lambda < 1$ the interaction between fermions is attractive. The ground state energy is independent of statistics, yet the interpretation for bosons is more involved: the ground state wave function (4) always describes repulsion between particles, despite the negative value of the potential energy for $\lambda < 1$. This paradox is due to the

singular character of interactions, namely the requirement that wave functions are zero for coinciding positions of the particles.

As can be seen in Fig. 1 both the kinetic and potential energies diverge as $\lambda \rightarrow 1/2$. It corresponds to the critical value of the coupling constant $g = \lambda(\lambda - 1) = -1/4$, below which particles fall to the center [1, 17]. For $\lambda < 1/2$ the expression (46) is not valid, since it predicts negative expectation value for the kinetic energy. The same applies to the potential energy (45). However the total energy is finite and analytic in the full range $\lambda > 0$ as follows from Eq. (44). Approaching the value $\lambda = 1/2$ from above the divergences of kinetic and potential energies cancel each other. In the interval $0 < \lambda < 1/2$ one cannot evaluate separately the potential energy using the Hellmann-Feynman theorem (45) due to the singular character of the ground-state wave function in this regime. To the best of our knowledge, this intriguing behaviour has not been noticed in the literature on the Calogero-Sutherland model despite the simple analysis based on use of the Hellmann-Feynman theorem.

VI. NUMERICAL RESULTS AND DISCUSSION

A. Monte Carlo method

Quantum Monte Carlo methods have been successfully applied to the investigation of the equation of state and correlation functions in a number of one-dimensional systems [18, 19, 20]. We resort to the Quantum Monte Carlo technique in order to evaluate multidimensional integrals Eqs. (5,7) numerically. This calculation of the correlation functions is exact in a statistical sense, the small statistical uncertainty can be reduced by increasing the length of the simulation runs. An advantage of the CSM is that the ground state wave function is known exactly and can be written in a simple explicit way, as given by Eq. (4), thus facilitating the calculations at zero temperature. Another important advantage of the CSM is related to the “sign problem” of fermionic Monte Carlo simulations. Here the permutation term can be factorized leading to a much simpler and efficient code than in three-dimensional systems, where the symmetrization of the fermionic wave function leads to the evaluation of Slater determinants. We use the Metropolis [21] algorithm for sampling the square of the wave function and generating a series of states (Markovian chain) having the desired probability distribution. The correlation functions are then calculated as averages over the Markovian chains. The calculation of the one-body density matrix $g_1(x)$ is performed by displacing a certain particle (let us choose x_1 as an example) by a distance x , so that $x'_1 = x_1 + x$ and averaging the ratio $\Phi(x'_1, x_2, \dots)/\Phi(x_1, x_2, \dots) = s_{B,F} \prod_{i \neq 1} |\sin(x'_1 - x_i)/\sin(x_1 - x_i)|^\lambda$ where $s_B = 1$ and $s_F = \prod_{i \neq 1} \text{sgn}(x'_1 - x_i)/\text{sgn}(x_1 - x_i)$. The average is performed with the probability distribution $|\Phi(x_1, \dots, x_N)|^2$. Similarly, we accumulate the pair distribution function by following the Markovian chain generated by the Metropolis algorithm and measuring the interparticle distance. The momentum distribution and static structure factor are calculated by means of Fourier transforms as defined by Eqs. (6,8). In what follows we present our results for the correlation functions in different interaction regimes.

B. One body density matrix

The results for the one-body density matrix are presented in Figs. 2 for Bose-Einstein and Fermi-Dirac statistics. Comparing the numerical results to Eqs. (30) and (31) we find that the asymptotic expansion works extremely well even for distances of the order of mean interparticle separation. It is important to note that the series (31) and (30) are asymptotic rather than convergent. The larger the distance x the more terms should be summed, while small distances are well described with only a few terms in the sum.

It is easy to see from Eq. (30) that the off-diagonal long-range order is absent as $g_1(x)$ always vanishes for large x . Still, for bosons and for small values of λ the leading term $g_1(x) \sim A^2/|2\pi x|^{\lambda/2}$ has a slow power-law decay, which is a manifestation of a quasi off-diagonal long-range order or *quasi-condensation*. This behaviour is shown in Figs. 2a-2b for small values of λ corresponding to weak interaction between particles. The smaller λ is, the more pronounced is the presence of a quasi-condensate. In this regime the one-body density matrix remains significantly different from zero even at distances much larger than the mean interparticle distance. The slowly decaying off-diagonal correlation in this regime is well described by the dominant term in the expansion (30). Oscillating corrections, corresponding to $m \geq 1$ terms in Eq. (30), decay rapidly on the scale of a few interparticle separations and are unimportant in this regime.

In this regime the off-diagonal correlations in fermionic systems are qualitatively different. For fermions, the one-body density matrix drops quickly from unity and oscillates around zero. In the fermionic case the main contribution to the long range asymptotics comes from the leading oscillating $m = 1$ term, Eq. (31).

With increasing λ the oscillating $m > 0$ terms in the long-range expansion of the bosonic one-body density matrix, Eq. (30), become important. Those contributions introduce oscillations corresponding to momenta $2mk_F$, $m = 1, 2, \dots$,

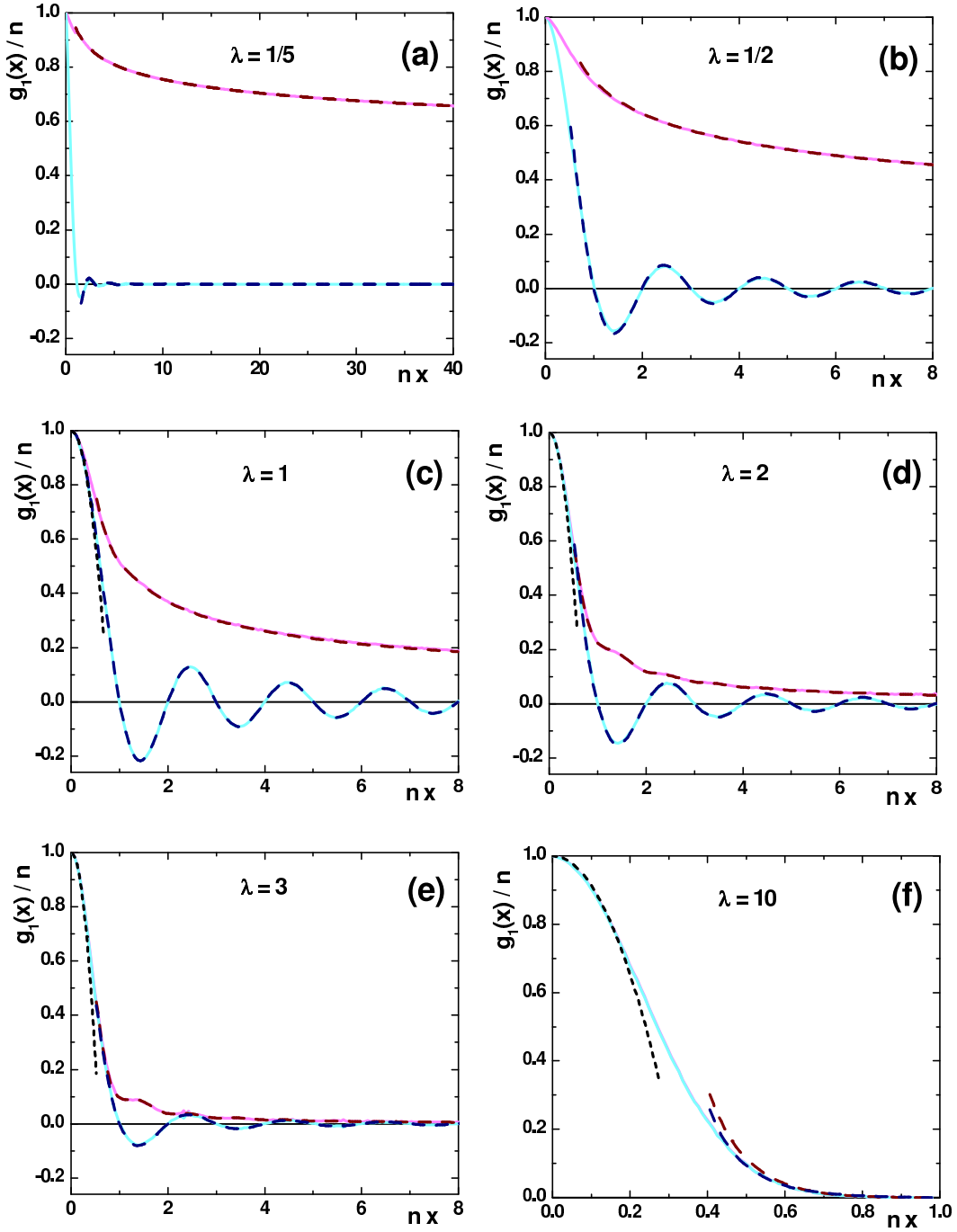


FIG. 2: (Color online) One-body density matrix $g_1(x)$ in the thermodynamic limit for different values of the interaction parameter λ . Solid lines: bosons (upper line); fermions (lower line). Long dashed lines: long range expansion for bosons, Eq. (30), (upper line); for fermions, Eq. (31), (lower line). Short dashed line (c,d,e,f): short-range expansion Eqs. (41,47). Note that the fermionic long-range expansion, Eq. (31), is exact for $\lambda = 1$ (c).

where $k_F = \pi n$ is the Fermi momentum. This behaviour can be attributed to the short-range order in the Calogero-Sutherland model, which becomes more important as the interaction strength increases. The results for intermediate values of interactions are depicted in Fig. 2b-2e.

For a bosonic system these short-range correlations are a manifestation of “fermionization”. Indeed, for $\lambda = 1$ the bosonic CSM becomes equivalent to a system of zero-range impenetrable bosons having the density correlations of free fermions. The correlation functions involving the phase are, however, drastically different and were the subject

of the classic works of Refs. [22, 23]. Recently there has been a revival of interest in this model [10, 16, 18, 24] due to realization of impenetrable bosons in several experiments with cold atoms [25]. For the fermionic CSM at $\lambda = 1$, the one-body density matrix is given by a standard expression for one-dimensional spinless fermions:

$$\frac{g_1^F(x)}{n} = \frac{\sin k_F x}{k_F x}, \quad \lambda = 1. \quad (48)$$

It is interesting to note that the asymptotic expansion (31) is exact for $\lambda = 1$. The results for the one-body density matrix at $\lambda = 1$ are shown in Fig. 2b both for free fermions and impenetrable bosons.

In the regime $\lambda > 1$ the system enters the quasi-crystal regime. The off-diagonal decay of the one-body density matrix is greatly enhanced. The oscillating terms in Eq. (30) become relevant and oscillations in $g_1^B(x)$ start to be visible (see Figs. 2d-2e) which reflects the appearance of the short range quasi-crystal order. For $\lambda = 2$ the bosonic one-body density matrix is known exactly [1] and is given by the expression

$$\frac{g_1^B(x)}{n} = \frac{\text{Si}(2k_F x)}{2k_F x}, \quad \lambda = 2, \quad (49)$$

where $\text{Si}(x)$ is the sine integral function. The expression (30) gives $g_1^B/n = \pi/4k_F x - \cos 2k_F x / 4k_F^2 x^2$ which coincides with the large x expansion of (49). We note that this behaviour of $g_1^B(x)$ is critical between long-range and short-range correlations, in the sense that the integral of $g_1^B(x)$ over space diverges for $\lambda < 2$ and converges for $\lambda > 2$. The description in terms of a quasi-condensate is applicable only in the long-range regime $\lambda < 2$.

For extremely strong interactions (for example, $\lambda = 10$, see Fig. 1) the potential energy dominates the total energy and quantum fluctuations are suppressed. In this regime the role of quantum statistics becomes irrelevant. This is due to the onset of the quasi-crystalline order, in which particles form a local crystal lattice so that the exchange effects of quantum statistics are irrelevant. As a result the one-body density matrices for bosons and fermions are very similar (see Fig. 2f). One finds that the fermionic one-body density matrix is positive in a large region and vanishes otherwise. The short-range expansion (41) describe quite well both fermionic and bosonic one-body density matrices. The quasi-crystal order is better probed by density correlations described in the subsection VID.

We have investigated the short-range behaviour of $g_1(x)$ numerically and we found a good agreement with the expression (41). The results are presented in Fig. 3. This figure shows the validity of the short-range expansion for different values of λ and allows to find the region of applicability of Eqs. (41,47). We see that the analytic short-range expansion holds in a larger range in the case of fermionic statistics as the omitted higher order terms of the short-range expansion are smaller in this case.

We point out that the coefficient c_2 in the short-range Taylor expansion has a minimum for $\lambda = 1$. This is clearly seen from numerical evaluation of the fermionic one-body density matrix presented in Fig. 3a. Interestingly, there are pairs of λ (for example, $\lambda=3/4$ and $\lambda=3/2$) with the same c_2 . The numerical results of the short-range behavior of a bosonic one-body density matrix are presented in Fig. 3b. The dominant c_2 term in the short-range expansion in this case is clearly seen for $\lambda = 1, 2, 3$, while for smaller values of λ the nonanalytic correction becomes comparable to the analytic contribution in the considered range $0.06 < nx < 0.5$.

We estimate the leading non analytic term and find that it goes as $|x|^{1+2\lambda}$ both for bosons and fermions. In the regime $\lambda < 1/2$ the non-analytic part in Eq. (41) provides the leading contribution $1 - g_1(z)/n \propto a(\lambda)|z|^{1+2\lambda}$. The point $\lambda = 1/2$ is very special. Indeed, the kinetic energy (46) diverges at this point (see Fig. 44), thus the Taylor coefficient c_2 is also divergent. However, this divergence is compensated by the divergence in the non-analytical term $a(\lambda)|x|^{1+2\lambda}$, which for $\lambda = 1/2$ is of the same order. We note that for $\lambda = 1$ the power of the non-analytical term becomes integer again and leads to a cubic correction, as was obtained by Olshanii *et al.* [16]. We prove numerically the presence of the non-analytic term proportional to $|x|^{1+2\lambda}$. The coefficient of this term can in principal be obtained from a best fit to the numerical data. We note that while the decay law is the same in bosonic and fermionic systems, the coefficient $a(\lambda)$ depends on the statistics and this leads to drastically different behaviour (e.g. $\lambda = 1/5$ in Figs. 3). The short-range non-analytical behaviour is related to the high momenta tails of the momentum distribution discussed in the next subsection.

C. Momentum distribution

The Fourier transformation (6) relates the one-body density matrix to the momentum distribution. The numerical results for this quantity are presented in Fig. 4 for the cases of bosonic and fermionic statistics.

In a system of weakly-interacting bosons, the power law decay of the one-body density matrix results in the divergence of the momentum distribution for small values of momenta: n_k is proportional to $|k|^{1-\lambda/2}$ as it follows from Eq. (32). This infrared divergence for small λ is reminiscent of Bose-Einstein condensation, *i.e.* macroscopic

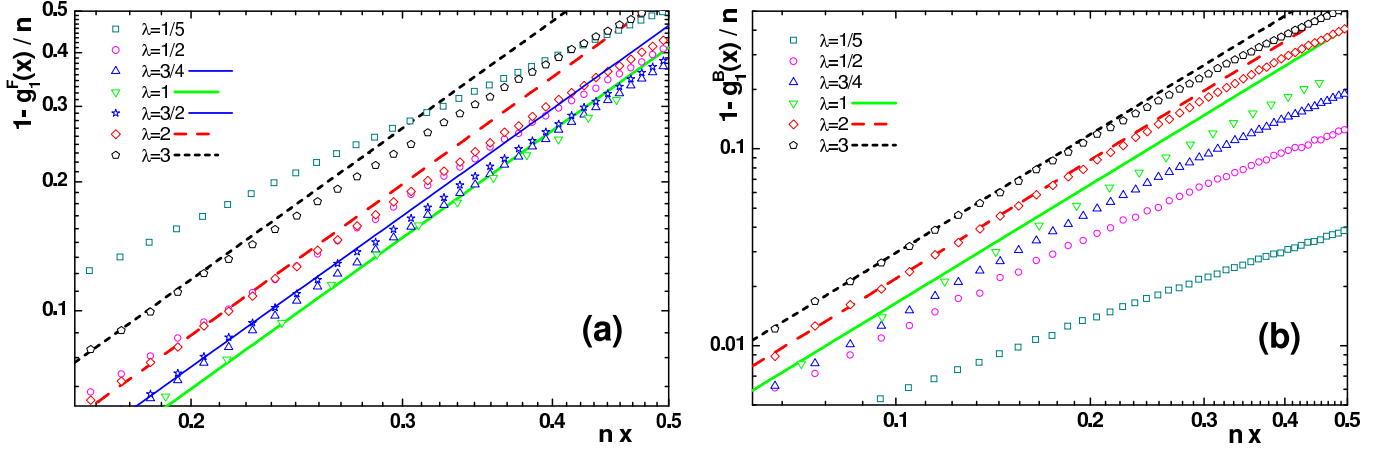


FIG. 3: (Color online) Short-range behavior of the bosonic (a) and fermionic (b) one-body density matrix $g_1(x)$ in the thermodynamic limit for different values of the interaction parameter λ . Symbols: results of the Monte Carlo simulations, lines: analytic part of the short-range expansion ($\lambda > 1$), Eqs. (41,47).

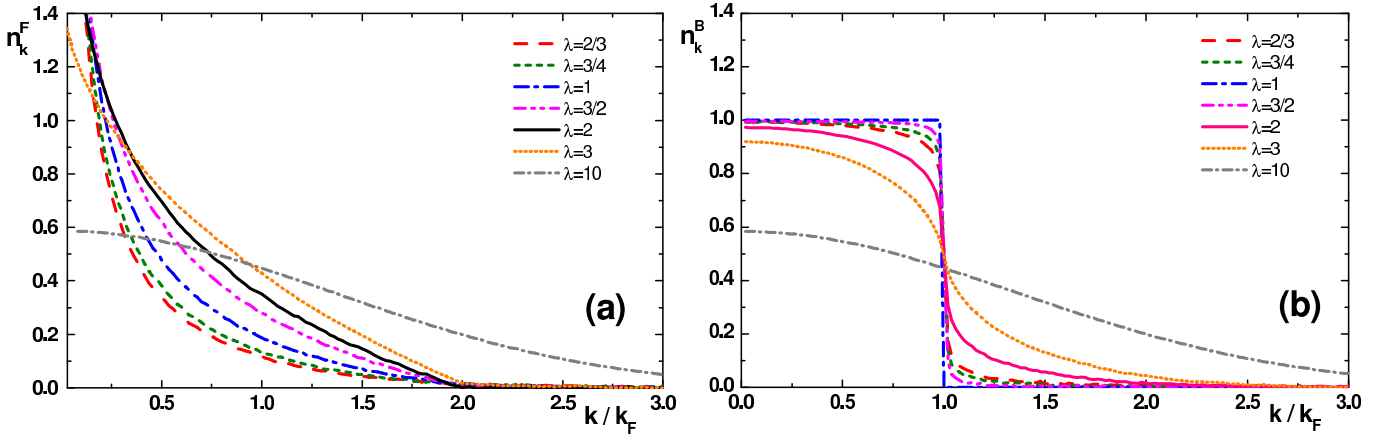


FIG. 4: (Color online) Momentum distributions for bosonic (a) and fermionic (b) CSM for different values of the interaction strength. Lines: in descending value at $k = 1.5k_F$: $\lambda = 10; 3; 2; 3/2; 1; 3/4; 2/3$.

occupation of the zero momentum state. The infrared divergence is present in the *quasi-condensate regime* for $\lambda < 2$. At $\lambda = 2$ the infrared divergence becomes logarithmic. From (49) we have an exact result [1] for the momentum distribution:

$$n_k^B = \begin{cases} \frac{1}{2} \ln \frac{2k_f}{|k|}, & |k| < 2k_f \\ 0, & |k| \geq 2k_f \end{cases}, \quad \lambda = 2. \quad (50)$$

We note that the logarithmic divergence for $\lambda = 2$ separates the power-law divergence for $\lambda < 2$ and a regular behaviour for $\lambda > 2$, so that $\lambda = 2$ is the critical value beyond which the quasi-condensation disappears.

The momentum distribution for a fermionic CSM is presented in Fig. 4(a). In the non-interacting case $\lambda = 1$ the momentum distribution of fermions is given by the step function at $k = \pm k_F$. For other values of λ the steps are absent and the momentum distribution has a power-law behaviour close to $\pm k_F$ described by Eq. (33). This is a characteristic of a Luttinger liquid behaviour present in the fermionic CSM. For very large λ the interactions completely destroy the Fermi surface and the momentum distribution is a decaying featureless function.

The behaviour of the momentum distribution for large momenta contains information about the physics at small length-scales. For instance, as we see from Eq. (50), the momentum distribution of bosons at $\lambda = 2$ has a cusp at $k = \pm 2k_F$. This discontinuity is a consequence of the oscillating term in the long-distance asymptotics, Eq. (30) or (49) and is a manifestation of the *short-range order*. Even for $\lambda < 2$ the presence of the short-range order shows itself

in weaker singularities of the momentum distribution for even multiples of k_F for bosons and odd multiples of k_F for fermions.

Apart from the special integer values of the interaction parameter λ (even for bosons, odd for fermions), the momentum distribution has a non-analytic high momenta tails decaying as $1/k^{2(1+\lambda)}$. At the special value $\lambda = 1/2$ the momentum distribution becomes broad, with tails decaying as $1/|k|^3$, which leads to a divergent mean kinetic energy $\propto \int k^2 n_k dk$ for $\lambda < 1/2$. In the case of zero-range impenetrable bosons ($\lambda = 1$) the Eq. (32) yields a $1/k^4$ ultraviolet behavior and has been discussed in [16].

The short-range order already present the one-body density matrix and the momentum distribution becomes evident in density correlations, which we consider in the next section.

D. Pair distribution function

The short-range order is best probed by calculating the pair distribution function $g_2(x)$ defined in Eq. (7). It gives the probability of finding two particle separated by a distance x . This function involves the absolute value of the ground state function and therefore is identical for bosons and fermions. The inverse square potential of the Calogero-Sutherland model prevents two particles from occupying the same position, so that $g_2(0) = 0$. For large interparticle separation the density correlations decouple and we have a general result $g_2(x) \rightarrow n^2, |x| \rightarrow \infty$. The pair distribution function has been studied in [9]. For distances larger than the mean interparticle separation the following result has been obtained

$$\frac{g_2(x)}{n^2} = 1 - \frac{1}{2\lambda(k_F x)^2} + 2 \sum_{m=1}^{\infty} \frac{d_m^2(\lambda)}{(2k_F x)^{2m^2/\lambda}} \cos(2mk_F x), \quad (51)$$

where

$$d_l(\lambda) = \frac{\prod_{a=1}^l \Gamma(1 + a/\lambda)}{\prod_{a=1}^{l-1} \Gamma(1 - a/\lambda)} = \Gamma\left(1 + \frac{l}{\lambda}\right) \prod_{a=1}^{l-1} \left(\frac{a}{\pi\lambda}\right) \sin\left(\frac{\pi a}{\lambda}\right) \Gamma^2\left(\frac{a}{\lambda}\right). \quad (52)$$

We have calculated the pair distribution function by using the Monte Carlo method and results are presented in Fig. 5. One sees that for small values of λ the pair distribution function goes smoothly from zero at short distances to the bulk constant at large distances. This is characteristic for a weakly interacting one-dimensional Bose gas or liquid [18]. As the regime of free fermions ($\lambda = 1$) is approached some oscillations become visible in the pair distribution. For this value of interactions the expression (51) gives the exact result:

$$\frac{g_2(x)}{n^2} = 1 - \frac{\sin^2 k_F x}{(k_F x)^2}, \quad \lambda = 1. \quad (53)$$

It is interesting to note that the powers characterizing the decay of the oscillating terms in the pair distribution, Eq. (51) and in the one-body density matrix of bosons, Eq. (30) are closely related. Employing the language of electronic systems these oscillating terms can be referred to as Friedel oscillations. It is a general feature that these oscillations become more pronounced as one moves to stronger interactions, since they arise due to the tendency of repelling particles to form a quasi-crystalline order. Friedel oscillations in the Calogero-Sutherland model have been discussed in [26] and similar oscillating behaviour of the same origin has also been observed in numerical simulations of the strongly interacting limit of one-dimensional bosons with delta-like interactions [18].

As interactions are made stronger the amplitude of oscillations become larger and number of visible oscillations is increased (see Fig. 5). Although the quantum fluctuations prohibit the formation of a “true” crystal, this behaviour of the Calogero-Sutherland model can still be described in terms of the local crystalline order as was pointed out by Krivnov and Ovchinnikov in [27]. In the next section we show how the quasi-crystal order manifests itself in the static structure factor.

E. Static structure factor

Density correlations characterized by the pair distribution function of the previous subsection are conveniently probed by measuring the static structure factor (8). It is related to the dynamic structure factor $S(k, \omega)$ which

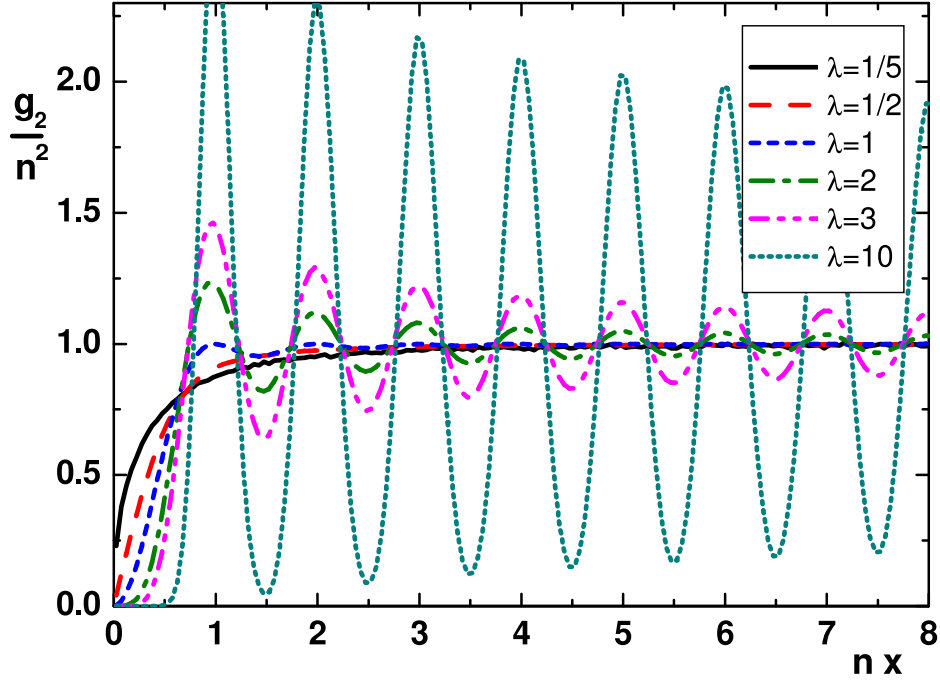


FIG. 5: (Color online) Pair distribution function for different values of the interaction strength λ . Lines: in descending order of the value at the first peak: $\lambda = 10; 3; 2; 1; 1/2, 1/5$.

characterizes the scattering cross-section of inelastic reactions where the scattering probe transfers momentum $\hbar k$ and energy $\hbar\omega$ to the system. In atomic gases it can be measured directly by the Bragg spectroscopy technique. By integrating out the ω dependence one obtains the static structure factor S_k . The numerical results for this quantity in the Calogero-Sutherland model are summarized in Fig. 6 for different interaction strengths.

The behaviour of the static structure factor for small momenta can be described by a hydrodynamic approach. The Feynman formula [28] $S_k = \hbar^2 k^2 / 2m\epsilon_k$ relates the static structure factor to the excitation spectrum exhausted by one branch ϵ_k . This is the case, when k is small and the excitations are phonons $\epsilon_k = \hbar kc$ with the speed of sound c . This leads to linear behavior for small momenta $S_k = \hbar|k|/2mc$. The speed of sound is related to the compressibility $\chi = mc^2 = n\partial\mu/\partial n$, where there chemical potential is be found from (44) as $\mu = \partial E/\partial N$. Thus we have

$$S_k = \frac{|k|}{2\lambda k_F}, \quad k \rightarrow 0, \quad (54)$$

in full agreement with the numerical results as can be seen in Fig. 6. Large momentum excitations behave as free particles $\epsilon_k = \hbar^2 k^2 / 2m$, so the static structure factor behaves as $S_k \rightarrow 1$ in the limit of large momenta.

In the regime of weak interactions $\lambda \rightarrow 0$, the static structure factor is a smooth function, which goes monotonically from 0 for $k = 0$ to unity for large values of momenta (see $\lambda = 1/5; 1/2$ in Fig. 6). This behaviour is very similar to that of rarefied weakly interacting gases [18]. The critical point at which a cusp at $k = 2k_F$ appears is $\lambda = 1$. For this critical value of λ the static structure factor can be written explicitly and takes a very simple form:

$$S_k = \begin{cases} \frac{|k|}{2k_F}, & |k| < 2k_F \\ 1, & |k| \geq 2k_F \end{cases}, \quad \lambda = 1. \quad (55)$$

The linear phononic behaviour continues until $|k| = 2k_F$, where the asymptotic constant value is reached. This special behavior is a result of averaging the dynamic form factor $S(k, \omega)$ over all excitation branches (see, for example [29]).

For $\lambda > 1$ a peak appears in the static structure factor indicating the onset of the quasi-crystalline order. In this regime the correlations between particles on short distance scale (of order several interparticle separations) become stronger. Similar physics was observed in numerical simulations of the metastable gas-like state in a short-range attractive potential (“super-Tonks-Girardeau” system [19]) or with dipole-dipole interactions [20].

By further increasing the strength of interactions, the peak at $k = \pm 2k_F$ becomes higher ($\lambda = 2; 3; 10$ in Fig. 6). For extremely strong interactions several peaks can be observed (see, as an example, $\lambda = 10$ in Fig. 6). The absence of

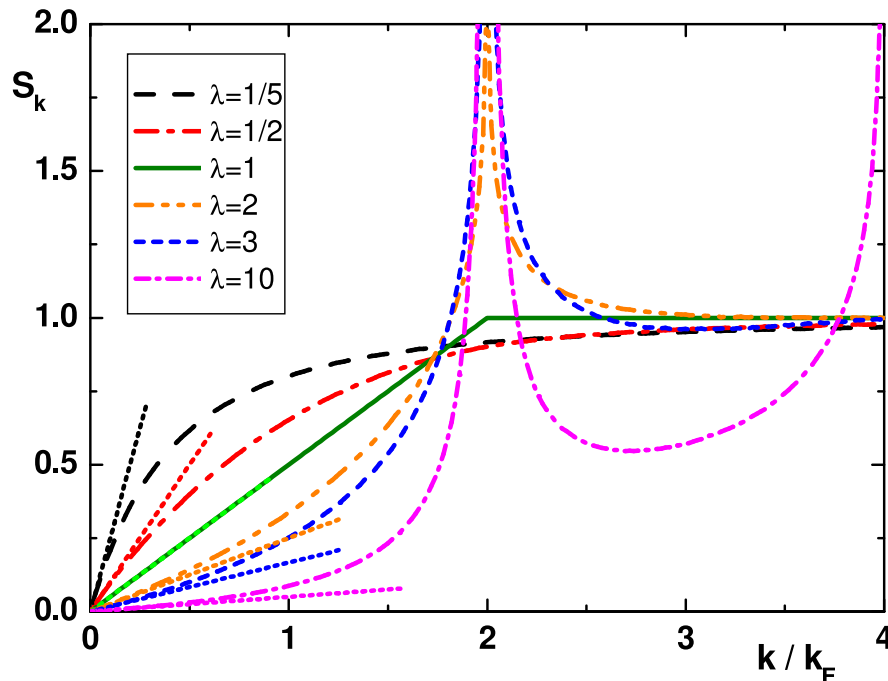


FIG. 6: (Color online) Static structure factor for different values of the interaction strength λ . Dashed lines: low momenta phononic behavior, Eq. (54). Interaction parameter (in order of decreasing slope at small k): $\lambda = 1/5; 1/2; 1; 2; 3; 10$.

coherence observed in the off-diagonal correlations in this regime allows us to conclude that for extremely large values of λ the Calogero-Sutherland model behaves as a lattice of classical particles, the one-dimensional Wigner crystal studied in [27].

VII. DISCUSSION AND CONCLUSIONS

The present study of the correlation functions of the Calogero-Sutherland model allows us to make conclusions about the dominant order, or rather, quasi-order present in the system as a function of the interaction parameter λ . We concentrate on the case of bosons and identify the following physical regimes at zero temperature.

For small values of λ the system is weakly interacting and stays in a gas-like (or liquid-like) state. There is a substantial degree of phase coherence in the system as follows from the slow decay of the off-diagonal correlations. For $\lambda < 2$ the bosonic momentum distribution n_k has an infrared divergence. This *quasi-condensate* regime is reminiscent of Bose-Einstein condensation, where the $k = 0$ state is macroscopically occupied. The divergence in the momentum distribution disappears completely for $\lambda > 2$, thus at this interaction value the Calogero-Sutherland system crosses over from a quasi-condensate to a non-condensed state for $\lambda = 2$ (see Fig. 7).

By increasing the strength of interactions one finds the appearance of strong positional ordering of particles (*quasi-crystal*) as indicated by the large amplitude of slowly decaying oscillations in the density-density correlation function $g_2(x)$. The critical value for this crossover from a liquid to a quasi-crystal state is estimated as $\lambda = 1$, where a singularity in the static structure S_k appears (see Fig. 7). For stronger interactions the particles form a one-dimensional Wigner crystal with a dominant crystalline order and absence of coherence.

The region $1 < \lambda < 2$ is very special as the one-body density matrix exhibits quasi off-diagonal long-range order while there is a quasi-crystalline order in the static structure factor. We denote this regime, where those two features are simultaneously present, as a *quasi-super-solid* in analogy with the super-solid state [30]. The word “quasi” is necessary while talking about the phase diagrams in a homogeneous one-dimensional system, as there is no true long-range order and no true phase transitions can take place in such systems [31]. The change of the regimes are actually crossovers. Indeed, the long-range asymptotics of the one-body density matrix (30) include both a slow power-law decay term as well as oscillating terms for *all* values of λ . The crossover takes place, when one kind of term becomes dominant over the other terms.

Aside from the question of quasi long-range order related to the behaviour of the correlation functions for large

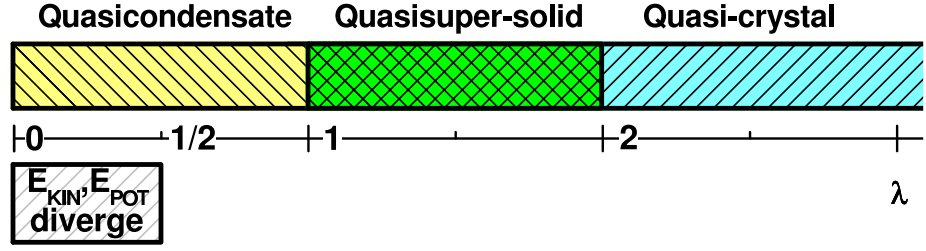


FIG. 7: (Color online) Phase diagram of the Calogero-Sutherland system. See text for the explanation.

distances on the scale of the interparticle spacing, we found interesting phenomena on the scale of the mean distance between particles. We found intriguing behaviour in the special region $\lambda \leq 1/2$ where both the potential and kinetic energies are divergent, while the total energy and the compressibility remain finite. The divergence first occurs for the critical value $\lambda = 1/2$ corresponding to the critical value of interactions beyond which the fall towards the center takes place [17].

The presented study of the correlation properties of the Calogero-Sutherland model in different physical regimes is of a high fundamental interest since this model provides one of the rare examples of integrable systems for which the correlation functions can be calculated exactly. Our description holds in physical regimes ranging from a weakly interacting gas to a strongly correlated crystal-like phase. We note that in an arbitrary one-dimensional gapless system supporting long-wavelength phonons, the ground state wave function can be approximately written as (4) [32]. This general description holds at distances where the hydrodynamic approach is applicable. So, the study of the Calogero-Sutherland model is important for understanding the long-wavelength properties of systems with linear low-momenta excitation spectra (also known as Luttinger liquids).

Apart from its theoretical importance, the Calogero-Sutherland model is relevant for several realistic physical systems. The classic example is provided by the compressible borders of Fractional Quantum Hall droplets [33]. The experiments on vicinal crystal surfaces [34] provide yet another physical realization of CSM. Recently, the particular case $\lambda = 1$ of bosonic CSM has been realized in the series of experiments [25] with tightly confined cold atomic gases.

It is important to stress that regardless of the absence of the true long-range order, the dominant quasi-order can reveal itself in mesoscopic confined systems due to their finite size. The study of physical regimes in mesoscopic systems confined in harmonic potentials are certainly of interest and will be considered in our future studies. Among other open questions one can name the time-dependent correlations as well as correlation functions of the Calogero-Sutherland model at finite temperature.

VIII. ACKNOWLEDGMENTS

D.M.G. would like to thank the University of Trento and the Institute of Spectroscopy for their hospitality during the work on this project. G.E.A. is grateful to LPTMS for hospitality. The work was supported by grants from the Ministère de la Recherche (grant ACI Nanoscience 201), Agence Nationale de la Recherche, IFRAF Ministero dell'Istruzione, dell'Università e della Ricerca (MIUR) and RFBR. We thank B. Jackson for reading the manuscript. LPTMS is the mixed research unit No. 8626 of CNRS and Université Paris Sud.

APPENDIX A: ANALYTICAL CONTINUATION OF A_n

We show how to perform an analytic continuation of the constant

$$A_m^2(\lambda) = \frac{\Gamma(m+1)}{\Gamma^2(m/2+1)} \prod_{c=1}^m \Gamma\left(\frac{m+c}{\lambda}\right) \prod_{a=1}^{m/2} \frac{\Gamma\left(1+\frac{a}{\lambda}\right)}{\Gamma\left(1+\frac{m/2+a}{\lambda}\right) \Gamma^2\left(\frac{m/2+a}{\lambda}\right)} \quad (\text{A1})$$

to $m = \lambda$. The first factor in the right hand side of this expression can be continued straightforwardly. Consider the logarithm of A_m^2

$$\ln\left(A_m^2 \frac{\Gamma^2(m/2+1)}{\Gamma(m+1)}\right) = \sum_{c=1}^m \ln \Gamma\left(\frac{m+c}{\lambda}\right) + \sum_{c=a}^{m/2} \left(\ln \Gamma\left(1+\frac{a}{\lambda}\right) - \ln \Gamma\left(1+\frac{m/2+a}{\lambda}\right) - 2 \ln \Gamma\left(\frac{m/2+a}{\lambda}\right) \right) \quad (\text{A2})$$

We use the following integral representation [35] for the logarithm of Euler's gamma function

$$\ln \Gamma(z) = \int_0^\infty \frac{dt}{t} \left(\frac{e^{-zt} - e^{-t}}{1 - e^{-t}} + (z-1)e^{-t} \right) \quad (\text{A3})$$

to represent each term in the right hand side of (A2). Summing finite geometric and arithmetic series under the integral we get

$$\ln \left(A_m^2 \frac{\Gamma^2(m/2+1)}{\Gamma(m+1)} \right) = \int_0^\infty \frac{dt}{t} e^{-t} \left(\frac{m^2}{2\lambda} + \frac{\left(1 - e^{-\frac{mt}{2\lambda}}\right)^2 - e^t \left(e^{-\frac{2mt}{\lambda}} - 3e^{-\frac{mt}{\lambda}} + 2e^{-\frac{mt}{2\lambda}}\right)}{(1 - e^{-t})(e^{t/\lambda} - 1)} \right), \quad (\text{A4})$$

which under replacement $m = \lambda$ yields the result (22).

The calculation in the fermionic case is similar. We have

$$C_m^2(\lambda) = \frac{\Gamma(m+1)}{\lambda} \frac{\Gamma^2\left(\frac{m+1}{2\lambda}\right)}{\Gamma^2\left(\frac{m+1}{2}\right)} \times \frac{\prod_{c=1}^m \Gamma\left(\frac{m+c}{2}\right) \prod_{a=1}^{\frac{m-1}{2}} \Gamma\left(1 + \frac{a}{\lambda}\right)}{\prod_{b=1}^{\frac{m+1}{2}} \Gamma\left(1 + \frac{m-1+2b}{2\lambda}\right) \Gamma^2\left(\frac{m-1+2b}{2\lambda}\right)}. \quad (\text{A5})$$

Taking the logarithm of this expression, using the integral representation (A3) and putting $m = \lambda$ yields the result (26).

-
- [1] B. Sutherland, J. Math. Phys. **12**, 246 (1971); **12**, 251 (1971); Phys. Rev. A **4**, 2019 (1971); **5**, 1372 (1972).
 - [2] F.D.M. Haldane, Phys. Rev. Lett. **67**, 937, (1991)
 - [3] F.J. Dyson, J. Math. Phys. **3**, 140, 157 (1962).
 - [4] B.D. Simons, P.A. Lee, and B.L. Altshuler, Phys. Rev. Lett. **70**, 4122 (1993); Nucl. Phys. B **409**, 487 (1993).
 - [5] B. Sutherland, Phys. Rev. B **45**, 907 (1992).
 - [6] F.D.M. Haldane and M.R. Zirnbauer, Phys. Rev. Lett. **71**, 4055 (1993).
 - [7] P.J. Forrester, Nucl. Phys. B **388**, 671 (1992); Phys. Lett. A **179**, 127 (1993);
 - [8] Z.N.C. Ha, Phys. Rev. Lett. **73**, 1574 (1994); P.J. Forrester and J.A. Zuk, Nucl. Phys. B **473**, 616 (1996); D. Serban, F. Lesage, V. Pasquier, Nucl. Phys. B **466**, 499 (1996).
 - [9] D. M. Gangardt and A. Kamenev, Nucl. Phys. B **610**, 578 (2001).
 - [10] D. M. Gangardt, J. Phys. A **37**, 9335 (2004).
 - [11] F.D.M. Haldane, Phys. Rev. Lett. **47**, 1840 (1981).
 - [12] J. Kurchan, J. Phys. A **24**, 4969 (1991).
 - [13] P.J. Forrester and N.S. Witte, Nagoya Math. J. **174**, 29 (2004).
 - [14] M. Mehta, *Random Matrices* (Academic Press, Boston, 1991), 2nd ed.
 - [15] M. Girardeau, J. Math. Phys. **1**, 516 (1960).
 - [16] M. Olshanii and V. Dunjko, Phys. Rev. Lett. **91** 090401 (2003)
 - [17] L. D. Landau, E. M. Lifshitz *Quantum Mechanics*, Elsevier (1981)
 - [18] G. E. Astrakharchik and S. Giorgini, Phys. Rev. A **68**, 031602(R) (2003).
 - [19] G.E. Astrakharchik, J. Boronat, J. Casulleras, S. Giorgini, Phys. Rev. Lett. **95**, 190407 (2005)
 - [20] A.S. Arkipov, G.E. Astrakharchik, A.V. Belikov, and Yu.E. Lozovik, Pis'ma v ZhETF **82**, iss.1, 41 (2005); cond-mat/0505700.
 - [21] N. Metropolis, A. W. Rosenbluth, M. N. Rosenbluth, A. H. Teller, and E. Teller, J. Chem. Phys., **21**, 1087 (1953)
 - [22] A. Lenard, J. Math. Phys. **5**, 930 (1964); J. Math. Phys. **7** 1268 (1966).
 - [23] H.G. Vaidya and C.A. Tracy, Phys. Rev. Lett. **42**, 3 (1979); J. Math. Phys. **20**, 2291 (1979).
 - [24] M. D. Girardeau and E. M. Wright Phys. Rev. Lett. **95**, 010406 (2005) A. Minguzzi and D. M. Gangardt Phys. Rev. Lett. **94**, 240404 (2005) M. A. Cazalilla Phys. Rev. A **67**, 053606 (2003)
 - [25] B. L. Tolra *et al.*, Phys. Rev. Lett. **92**, 190401 (2004); B. Paredes *et al.* Nature **429**, 277 (2004); T. Kinoshita, T. Wenger, D. S. Weiss, Science **305**, 1125 (2004).
 - [26] S.M. Nishigaki, D.M. Gangardt and A. Kamenev, J. Phys. A **36**, 3137 (2003).
 - [27] V.Ya. Krivnov and A.A. Ovchinnikov, Sov. Phys. JETP **55**, 162 (1982).
 - [28] R. P. Feynman, Phys. Rev. **94**, 262 (1954)
 - [29] L. P. Pitaevskii and S. Stringari, *Bose-Einstein Condensation*, Oxford University Press, Oxford (2003)
 - [30] A.F. Andreev and I.M. Lifshitz, Sov. Phys. JETP **29**, 1107 (1969).
 - [31] L. D. Landau, E. M. Lifshitz *Statistical Physics, Part 1* Elsevier (1980)
 - [32] L. Reatto and G. V. Chester, Phys. Rev. **155**, 88 (1967)
 - [33] M. Stone and M.P.A. Fisher, J. of Mod. Phys. **8**, 2539 (1994)
 - [34] T.L. Einstein, Ann. Henri Poincaré **4**, S811-24 (2003)
 - [35] I.S. Gradshteyn, I.M. Ryzhik, *Table of Integrals, Series, and Products* (Academic Press, Boston, 2000), 6th ed.